Journal of Biological Dynamics

ISSN: 1751-3758 (Print) 1751-3766 (Online) Journal homepage: http://www.tandfonline.com/loi/tjbd20

Glioblastoma brain tumours: estimating the time from brain tumour initiation and resolution of a patient survival anomaly after similar treatment protocols

J. D. Murray

To cite this article: J. D. Murray (2012) Glioblastoma brain tumours: estimating the time from brain tumour initiation and resolution of a patient survival anomaly after similar treatment protocols, Journal of Biological Dynamics, 6:sup2, 118-127, DOI: 10.1080/17513758.2012.678392

To link to this article: https://doi.org/10.1080/17513758.2012.678392

Journal of Biological Dynamics
Vol. 6, Suppl. 2, September 2012, 118–127

Taylor & Francis
Taylor & Francis Group

Glioblastoma brain tumours: estimating the time from brain tumour initiation and resolution of a patient survival anomaly after similar treatment protocols

J.D. Murray[a,b,c]*

[a]*Applied and Computational Mathematics, Princeton University, Princeton, NJ, USA;* [b]*Ecology and Evolutionary Biology, Princeton University, Princeton, NJ, USA;* [c]*Centre for Mathematical Biology, Mathematical Institute, University of Oxford, Oxford, UK*

(*Received 31 December 2011; final version received 6 March 2012*)

A practical mathematical model for glioblastomas (brain tumours), which incorporates the two key parameters of tumour growth, namely the cancer cell diffusion and the cell proliferation rate, has been shown to be clinically useful and predictive. Previous studies explain why multifocal recurrence is inevitable and show how various treatment scenarios have been incorporated in the model. In most tumours, it is not known when the cancer started. Based on patient *in vivo* parameters, obtained from two brain scans, it is shown how to estimate the time, after initial detection, when the tumour started. This is an input of potential importance in any future controlled clinical study of any connection between cell phone radiation and brain tumour incidence. It is also used to estimate more accurately survival times from detection. Finally, based on patient parameters, the solution of the model equation of the tumour growth helps to explain why certain patients live longer than others after similar treatment protocols specifically surgical resection (removal) and irradiation.

Keywords: glioblastoma; brain tumour; tumour initiation; survival anomaly; imaging enhancement

1. Introduction

Glioblastomas (gliomas) are the most aggressive brain tumours. Irrespective of any of the current treatment protocols, they are always fatal with a median life expectancy of 9–12 months from detection [12]. This work particularly emphasizes the multifocal recurrence after surgical resection (removal) the reason for which is clear from the model initially proposed ([4], see [9] for a detailed survey). Gliomas make up more than 50% of all brain tumours. The evolution of medical imaging has increased the detection of gliomas but cannot define sufficiently the degree of diffuse invasion of the tumour cells peripheral to the bulk of the tumour mass. The various treatment protocols such as surgical resection, radiation and chemotherapy cannot effect a cure but can frequently extend survival time. Treatment efficacy depends on various factors such as where the tumour is located in the brain and, as shown below, what are crucially important, the size of the key tumour parameters, the growth rate (cell proliferation) and the diffusion rate (cell motility).

*Email: jdmurray@princeton.edu; james.murray@maths.ox.ac.uk

ISSN 1751-3758 print/ISSN 1751-3766 online

http://dx.doi.org/10.1080/17513758.2012.678392
http://www.tandfonline.com

A practical basic mathematical model for quantifying the effect of intervention strategies for the control of gliomas by chemotherapy was first proposed in [20] and for resection in [22]. Subsequent studies [13–18] refined the model for anatomically correct brains and certain predictions were confirmed by scans and often by autopsy. The results quantitatively confirm that gliomas always diffuse and cannot be cured by resection alone, surgically or radiologically, irrespective of the degree of malignancy. The developments of this model have proved medically illuminating and clinically practical [11,18].

The model analyses also predicted the behaviour of untreated high-, intermediate- and low-grade tumours and showed [22] the behaviour of surgically treated high-grade gliomas to a degree of accuracy which had not been possible *in vivo* with statistical significant probability even with groups of more than 50 real patients [5]. The work by Kelly *et al.* [5], Swanson *et al.* [14] and Woodward *et al.* [22] clearly demonstrated why tumour recurrence cannot be other than multifocal while in [1] the limitations of existing imaging techniques were reconfirmed: these limitations still exist. Cruywagen *et al.* [4] were the first to demonstrate that cancer cell diffusion, mainly ignored up to that time, is a major component of glioma growth.

A major advance in the practical application of the model briefly described in detail below was the availability of the brain web atlas [3]. This allowed the model to be applied to anatomically correct brains (see [9] for a full discussion and review which encompasses anatomically correct brains). Among other things, the brain web made it possible to refine the gross anatomic boundaries and to vary the degree of motility of glioma cells in grey or white matter; these are biologically significant [13,14]. The availability of correlated CT, MRI and needle biopsies allowed comparison of the more refined model with applications to real patients [5,10,17,18]. Current intervention therapies can be similarly incorporated, as in previous studies, into the model equations (1) and (2), for anatomically correct brains by including a term on the right-hand side which mimics resection, periodic chemotherapy and periodic radiation.

With the increasing discussion and concern of the possible increase in brain tumours as a consequence of the ever expanding use of cell phones, it is inevitable that serious clinical studies will be carried out in the relatively near future. The serious effect cell phone radiation has on plant growth has been clearly demonstrated [19]. It was shown that a single 2 h exposure to radiation emitted at 105 GHz from a (GSM) cell phone resulted in considerable growth deformity. An increase in brain glucose in the region closest to the cell phone antenna has also been reported [21]. To date, no study has definitively stated that brain tumours can arise from prolonged use of cell phones. In any scientific clinical trial, it will be useful information to know when a tumour started, how fast it grows and where it is in the brain outside of what can be detected with current imaging procedures. We show below how the model provides a means of estimating the time from tumour initiation to detection and also life expectancy from tumour detection for individual patients. Analysis of the model also helps to explain a long-standing anomaly as to why some patients undergoing similar treatments live longer than others.

2. Model for glioblastoma (brain tumour) growth

The basic models (see the review [9]) considered the brain to be homogeneous, only bounded externally by the arachnoid and internally by the ependyma of the ventricles. With the BrainWeb atlas [3], it was possible to show how a virtual glioma grows and migrates in any of the three standard planes (coronal, sagittal and axial or horizontal) and to demonstrate how a true three-dimensional representation of a glioma would allow each 1 mm thick slice of brain to interact with grey and white matter in adjacent planes [13].

The mathematical model which encompasses the two key elements in the growth of tumours, namely the invasive diffusive properties of the cancer cells and their growth rate, is qualitatively

given by the equation:

$$\text{Rate of change of tumour cell density} = \text{diffusion (invasion) of tumour cells} + \text{net proliferationof tumour cells.} \quad (1)$$

The mathematical form which quantifies Equation (1) is

$$\frac{\partial c}{\partial t} = \nabla \cdot D(x)\nabla c + \rho c, \quad (2)$$

where the various terms in this equation are defined as $c(\mathbf{x}, t)$ is the glioma cell density, measured in cells/mm^3; it is a function of the position $\mathbf{x}$ in the brain at time t measured in months. $D(\mathbf{x})$ is the cell diffusion (invasion), measured in mm^2/month, which quantifies the invasiveness of the cancer cells at position $\mathbf{x}$ in the brain. ρ is the net proliferation rate (per month) of the cancer cells which gives the cell turnover time as $(\log 2)/\rho$ (months).

This equation was solved numerically with zero flux of cells across the brain boundaries and an initial condition at time $t = 0$ of the distribution of tumour cells, denoted by N, before diffusion begins. There is no agreement as to how large the tumour has to grow as a local mass before it starts to diffuse. Numbers from 2 to 4000 cells/mm^3 have been suggested. As seen below, it is the ratio of the imaging detectable concentration, denoted by c_1, to N which appears in the solution (Equation (4)). In the simulations for tumour initiation time and life expectancy, a range of such ratios from 4000 to 80,000 cells/mm^3 was used.

With two individual patient brain scans, such as enhanced CT, MRI and others, the key model parameters, namely the diffusion, D, and the cell growth, ρ, can be calculated [14]. With these parameter values, it is possible to predict the growth of such brain tumours and, importantly, estimate key aspects of the tumour's growth and response of individual patients to different treatment protocols *prior* to their use. One study has been carried out in the case of irradiation [11].

Simulations of an anatomically correct brain highlight the limitations of current imaging techniques as clearly shown in [14]. Figure 1 is a computed solution of the model equation (2) in an anatomically correct brain: it shows the detectable tumour at death and the spread of the tumour cells beyond what can be detected by the most accurate current CT or MRI imaging techniques. Thus, simulations of the model greatly enhance current imaging techniques to whatever level of cancer cell density is required. The model analysis [14] shows how fast the tumour grows and, importantly, where in the brain.

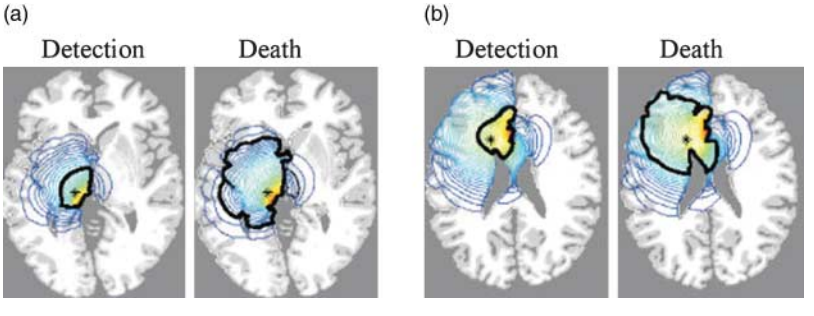

Figure 1. Computed solutions of Equation (2) in a three-dimensional anatomically accurate brain. The horizontal section of the virtual human brain through the site of the original tumour is shown (+ in (a), ∗ in (b)). The left image in each is the tumour at diagnosis while the right image is the same tumour at time of death. The thick black contour defines the edge of the tumour that can be detected by enhanced CT. The blue contours outside this black line represent lines of constant cancer cell densities peripheral to the imaging limits. (a) Tumour in grey matter: the time from diagnosis to death is approximately 8 months. (b) Tumour in white matter: the time from diagnosis to death is approximately 5 months (Figures extracted from [14]).

3. Estimating *in vivo* patient survival time

The solutions of the model equation provide life expectancy estimates for individual patients and, crucially in the event of a scientific clinical study, estimates of how long the tumour has been growing before it is detected. The procedure is to estimate the parameter values for each patient to obtain the average diffusion coefficient and the average growth rate as in [14]. There is a lower threshold of detection of cancer cells with all imaging techniques, whether CT or MRI, such as T1Gd and T2 imaging, or microscopic studies. This is an input in solving the equation. A threshold concentration estimate of 8000 cells/mm^3 was used [1,14]. Depending on the scanning technique, this value can be lower or higher. To use the predictive potential of the mathematical model (2), the serial imaging of the tumour is used to calculate its volume from which the volume of an equivalent sphere with radius r, namely $4\pi r^3/3$, is calculated. The model then considers an equivalent radially symmetric tumour with a constant diffusion coefficient, based on averaging the values from the imaging. For such a spherical tumour growth, Equation (2) becomes

$$\frac{\partial c}{\partial t} = D\left[\frac{\partial^2 c}{\partial r^2} + \frac{2}{r}\frac{\partial c}{\partial r}\right] + \rho c. \tag{3}$$

Initially, at time $t = 0$, there is a concentrated number of cancer cells, N cells/mm^3 at $r = 0$, in which case the solution of Equation (3) is given by

$$c(r,t) = \frac{N\ \exp(\rho t - r^2/4Dt)}{8(\pi Dt)^{3/2}}. \tag{4}$$

If the smallest level of image detection is denoted by c_1 cells/mm^3, then the radius, r, of the tumour for this cell density is, on solving for r,

$$r = 2t\sqrt{D\rho}\sqrt{1 - \frac{1}{\rho t}\log\left(\frac{c_1}{N}(4\pi Dt)^{3/2}\right)}. \tag{5}$$

For large time, t, the solution (5) gives (see, for example, [9,18]) the approximate radius of the detectable tumour and the velocity of growth, v, as

$$r = 2t\sqrt{D\rho} \Rightarrow v = \frac{r}{t} = 2\sqrt{D\rho}. \tag{6}$$

That is, the equivalent radial growth is linear in time, a finding medically confirmed [7].

If we consider detection is when the spherical equivalent tumour volume is typically of radius 15 mm and that death occurs when the radius is 30 mm [9,13,14], the approximate survival time from detection, in the absence of any treatments, is given, from Equation (6), by

$$\text{Survival time (months)} = t_{\text{survival}} = t_{r=30} - t_{r=15} = \frac{7.5}{\sqrt{D\rho}}. \tag{7}$$

Typical growth rates, ρ, and diffusion values, D, vary quite widely, although most are approximately in the range $\rho = 0.1$–5/month and $D = 0.1$–$8\,\text{mm}^2$/month. The ranges of parameter values for nine patients [11] with glioblastomas were $D = 0.55$–$4.23\,\text{mm}^2$/month and $\rho = 0.3$–4.19/month: the medians are $D = 0.9\,\text{mm}^2$/month and $\rho = 1.16$/month. These give a median survival time without any treatment for 7.34 months. The patients in this study, however, underwent irradiation treatment and survived considerably longer.

Survival time, however, depends on where the tumour is mainly situated. If it is primarily in the grey area of the thalamus, for example, the diffusion is smaller and so the survival time is longer, as is clear from Equation (7).

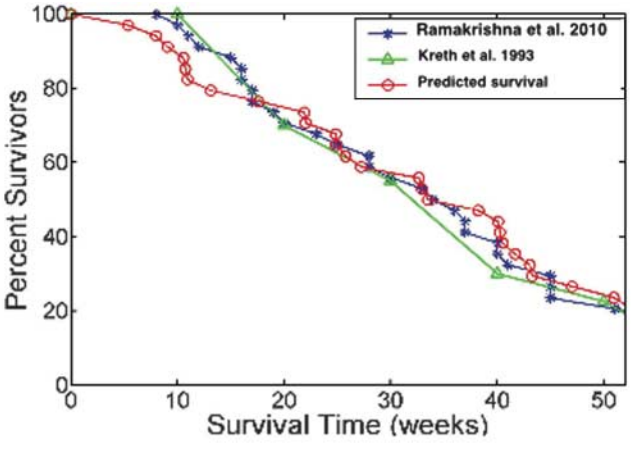

2

Figure 2. Survival time calculated from the model when compared with that from patient data (data extracted and updated from [6,10,22]).

Modelling the various treatment scenarios involves adding terms on the right-hand side of Equation (3) which mimic the specific therapy considered. Crucially, from a medical point of view, the model has been used to quantify the effect of different treatment efficacies for individual patients *prior* to their use. Incorporating periodic chemotherapy has been studied [15,20]. Here, Equation (1) is modified by a further (negative) term on the right-hand side which quantifies the periodic reduction in growth as a consequence of the chemotherapy or irradiation. Incorporating subtotal and total tumour resection in patient survival was discussed in [22]. This involves visually excising a given volume of the tumour in the model simulations. The predictions compared well with the patient data [6]. The modelling study [22] predicted patient survival rates which, considering the basic aspect of that model, compared surprisingly accurately with the extant data at the time, some of which has recently been published [10] (Figure 2), and even more so in the study using the anatomically correct brain [18]. A full review and how such treatment protocols are incorporated are given in [9].

4. Estimating the time from tumour initiation to detection and survival times from detection

Irrespective of the possible cell phone use connection, knowing when a brain tumour started, as opposed to just when it was detected, is information which provides a window of time which could provide important clues as to its origin and pose relevant questions in any major scientific clinical study. Determining when a tumour started is an unsolved problem with most cancers. In the case of glioma brain tumours, detection is, on average, when the tumour volume is approximately equal to an equivalent sphere of radius 3 cm in diameter but this also depends on the imaging technique used and where the tumour is in the brain. It is essential therefore to be able to incorporate in any realistic formula for the time from tumour initiation, such as the radius of the equivalent sphere at detection, the *in vivo* cancer cell growth rate and diffusivity of the cells.

As a first approximation, the expression (6) gives the radius of the tumour and its velocity as a function of the diffusion coefficient and growth rate but only for large times. This, however, is only valid for sufficiently large times and although useful for calculating the approximate life expectancy since it is after the tumour has been detected, it is insufficiently accurate to back extrapolate to when the tumour started. It significantly underestimates the time.

A more accurate estimate is obtained using the exact solution (4) for the cell concentration as a function of time. If $c_1(r,t)$ denotes the outermost cancer cell density level of detection when the tumour has an equivalent sphere radius of r then the time it takes for an initial density of N cells to grow and diffuse is given by the solution t of Equation (5) for given r, c_1, N, D and ρ. There is no analytical solution of this equation but it is easy to program MATLAB, for example, to obtain the value for t for any given r, c_1, N, D and ρ, of which all, except N, are determined from *in vivo* patient scans. This gives the time to initiation for all radii r, not only the radius at the smallest detection level but, importantly, whenever the tumour is first observed. It also gives a more accurate estimate for the survival time than Equation (7) by assigning the radius to be 3 cm or whatever value is deemed more accurate from the scanning procedure used.

It is not known how many cancer cells, N, are required before they start to diffuse nor an accurate value for the detection level c_1. In [14,15,22], a value of 8000 cells/mm^3 was used based on cell size estimates. To show the effect on tumour initiation time, by way of example we chose c_1/N in Equation (5) to be in one case 4000 cells/mm^3 and in the other 80,000 cells/mm^3. Figure 3 shows the times from initiation to detection for a typical range of growth rates and diffusion coefficients for each of these threshold values.

It is clear from Figure 3 that for large diffusion rates there is little variation in the time from initiation for a given reproduction rate. For small diffusion rates, however, it is significant, as they are also, in increasing life expectancy as shown below. The effect of a 20-fold change in the ratio c_1/N is also very small.

Survival time without treatment for patient values of diffusion, D, and growth rate, ρ, is given by Equation (5) on solving for the time t for the equivalent lethal radius of the tumour, namely $r = 3$ cm. For a range of diffusion values and growth rates, Figure 4 shows this survival time from initiation and from detection at a representative $r = 1.5$ cm.

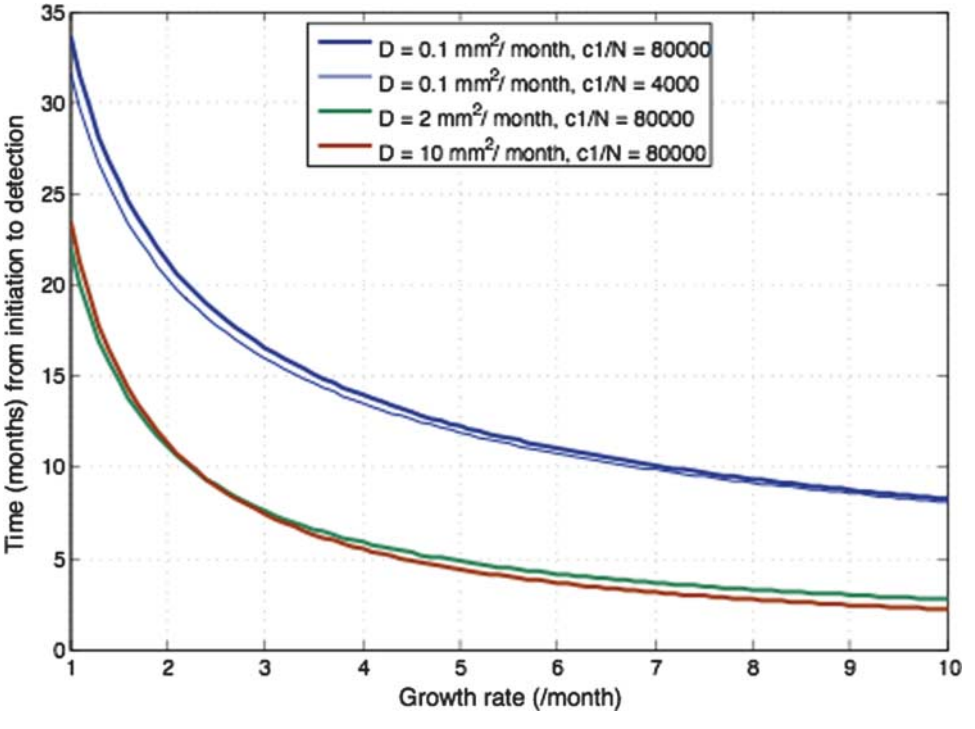

Figure 3. Time from tumour initiation to detection at an equivalent spherical diameter of 3 cm for a wide range of diffusion coefficients. For $D = 0.1$ mm^2/month two values are taken for the ratio c_1/N of detectable density, c_1, to initial cell density, N.

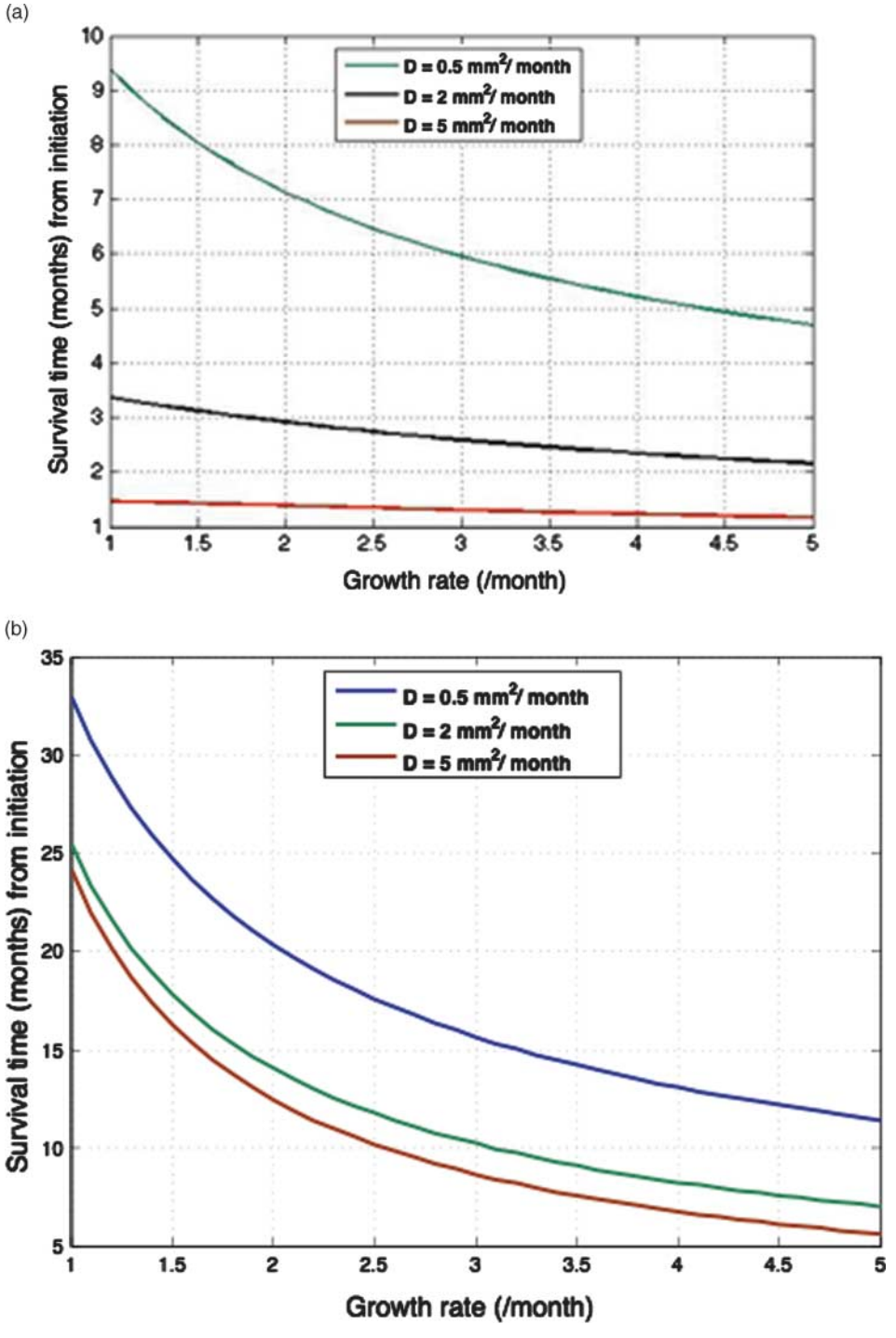

Figure 4. (a) Survival time from detection for a typical range of diffusion coefficients. The ratio c_1/N of detectable density, c_1, to initial cell density, N, used is 80,000 cells/mm^3. (b) Survival time from initiation. The major differences in survival time with reference to diffusion are when the diffusion coefficient is small. For larger diffusion values, the survival time is almost irrespective of the growth rate.

Figure 4(b) illustrates two important aspects. Diffusion coefficients larger than approximately $2\,\text{mm}^2/\text{month}$ have little effect on the time from tumour initiation. With these values, the growth rate has a more important role. A greatly reduced value of the ratio c_1/N of the detectable density, c_1, to initial cell, N, of $4000\,\text{cells}/\text{mm}^3$, that is only 5% of the $80{,}000\,\text{cells}/\text{mm}^3$, has little effect: even at low growth rates the maximum difference in time is only of the order of 6%.

5. Survival anomaly: why do some patients survive longer than others with the same treatment protocol?

Generally, resection surgery and irradiation try to target as much of the tumour as can be determined from brain scans. The solution (4) of the radially symmetric model equation (3) shows there is no 'edge' to the tumour: the cancer cell density at any given time and position is exponentially small. However, the two parameters, diffusion, D, and proliferation rate, ρ, play major roles in the actual cancer cell distribution as a function of distance from the initiation site. Equation (3) has been studied in another context [8], and it was shown that the qualitative steepness of the tumour has a maximum gradient, $G_{\max}$, and an approximate tumour width, R_{width}, in the equivalent spherical tumour, given by

$$G_{\max} \approx \frac{1}{8}\sqrt{\frac{\rho}{D}}, \quad R_{\text{width}} \approx 16\sqrt{\frac{D}{\rho}}. \tag{8}$$

From these, the smaller the diffusion parameter the steeper the gradient and therefore the more contained the tumour. Figure 5 illustrates these solution attributes.

From Figure 5 and Equation (8), it is clear how much more accurate a surgical resection (or irradiation) can be effected if the diffusion coefficient is small. The brain scan in this case can indicate more accurately where the major part of the tumour lies and hence more of the tumour can be excised when compared with a tumour with a larger diffusion coefficient. With the parameter values in Figure 5, the maximum gradients are, respectively, 0.4, 0.18 and 0.13/mm, while the approximate widths are, respectively, 5, 11 and 16 mm. After resection, or irradiation, there are, therefore, fewer cancer cells to initiate the observed multifocal growth and hence the time to subsequent detection will be longer. This is only one aspect of patient survival. Another important

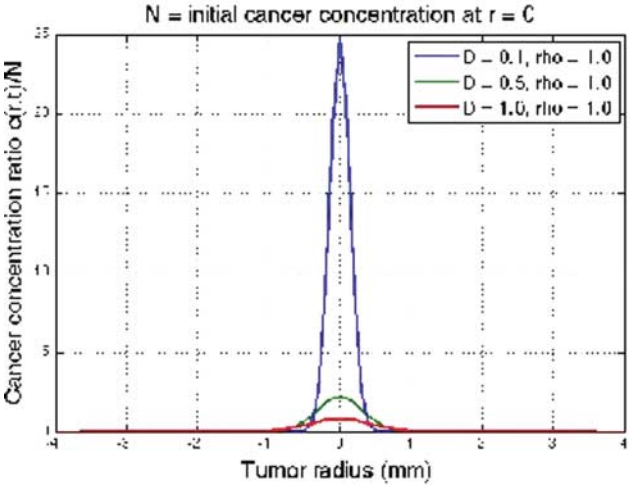

Figure 5. Cancer cell concentration solutions of Equation (3) for a range of diffusion coefficients D mm^2/month and proliferation rate $\rho = 1.0/\text{month}$.

input is where the tumour is in the brain. However, for tumours in approximately the same area, the predictions here give a quantitative indication of the possible efficacy of different treatment protocols for the individual patient based on their tumour growth parameters and, with the exact solution of the model equation, a more accurate estimate of patient survival.

Brain tumours in children can exhibit quite different characteristics which in some cases can benefit from gross total resection. In one study [2] of seven cases, the children had no evidence of recurrence after 49–136 months. From the data presented in Figures 2–5, it is possible that these children's tumours had very low diffusion rates thereby allowing the tumour to be detected and more completely resected before there had been significant diffusion.

6. Discussion

The mathematical model described quantifies the extent of tumourous invasion of individual gliomas to a degree beyond the limits of present medical imaging, including microscopy. There is now a considerable body of *in vivo* research which confirms the quantitative predictions of the model given by Equation (2). The solutions and applications enhance the reality of imaging and highlight the inadequacies and limitations of current therapies. Most research on the control of tumours is centred around specific treatments to reduce the growth of the tumour. The work described here provides one further piece of practical information for glioblastoma brain tumours which is not normally available for any tumour growth, namely an estimate for the time from initiation to detection of the tumour. This could possibly assist in recalling an event or situation that could provide some clue as to the possible reason for such an aggressive tumour. The model solutions also contribute to explaining the medical anomaly of why some patients whose tumours are resected or irradiated live longer than others.

It is a privilege to dedicate an article in this issue to Simon Levin, with whom I have had the good fortune of working as a good friend and colleague for several decades. His thoughtfulness, encouragement, enthusiasm and remarkable innovative scholarship have been, for me, and many others, an enriching, motivating and enjoyable experience.

References

[1] P.K. Burgess, P.M. Kulesa, J.D. Murray, and E.C. Alvord, *The interaction of growth rates and diffusion coefficients in a three-dimensional mathematical model of gliomas*, J. Neuropath. Exp. Neurol. 56 (1997), pp. 704–713.

[2] J.W. Campbell, I.F. Pollack, A.J. Martinez, and B. Shultz, *High-grade astrocytomas in children: Radiologically complete resection in association with an excellent long-term prognosis*. Neurosurgery 38 (1996), pp. 258–264.

[3] C.A. Cocosco, V. Kollokian, R.K.-S. Kwan, and A.C. Evans, *BrainWeb: Online interface to a 3D MRI simulated brain database*, NeuroImage 5(4, part 2/4, S425) (1997). Proceedings of the 3rd International Conference on Functional Mapping of the Human Brain, Copenhagen 1997 (http://www.bic.mni.mcgill.ca/brainweb/).

[4] G.C. Cruywagen, D.E. Woodward, P. Tracqui, G.T. Bartoo, J.D. Murray, and E.C. Alvord, *The modelling of diffusive tumors*, J. Biol. Syst. 3 (1995), pp. 937–945.

[5] P.J. Kelly, C. Daumas-Duport, D.B. Kispert, *et al.*, *Imaging-based stereotaxic serial biopsies in untreated intracranial glial neoplasms*, J. Neurosurg. 66 (1987), pp. 865–874.

[6] F.W. Kreth, P.C. Warnke, R. Scheremet, and C.B. Ostertag, *Surgical resection and radiation therapy versus biopsy and radiation therapy in the treatment of glioblastoma multiforme*, J. Neurosurg. 78 (1993), pp. 762–766.

[7] E. Mandonnet, J.Y. Delattre, M.L. Tanguy, K.R. Swanson, A.F. Carpentier, H. Duffau, P. Cornu, R. Van Effenterre, E.C. Alvord, and L. Capelle, *Continuous growth of mean tumor diameter in a subset of grade II gliomas.* Ann. Neurol. 53 (2003), pp. 524–528.

[8] J.D. Murray, *Mathematical Biology*, 1st ed., Springer, New York, 1989.

[9] J. D. Murray, *Mathematical Biology: II. Spatial Models and Biomedical Applications*, 3rd ed., Springer, New York, 2003.

[10] Ramakrishna, J. Barber, G. Kennedy, R.H. Rizvi Win, G.A. Ojemann, M.S. Berger, A.M. Spence, and R.C. Rostomily, *Imaging features of invasion and preoperative and postoperative tumor burden in previously untreated glioblastomas: Correlation with survival*, Surg. Neurol. Int. 1 (2010). Available at http://dx.doi.org/10.4103/2152-7806.68337.

[11] R. Rockne, J.K. Rockhill, M. Mrugala, A.M. Spence, I. Kalet, K. Hendrickson, A. Lai, T. Cloughesy, E.C. Alvord, and K.R. Swanson, *Predicting the efficacy of radiotherapy in individual glioblastoma patients in vivo: A mathematical modeling approach*, Phys. Med. Biol. 55 (2010), pp. 3271–3285.

[12] D.L. Silbergeld, R.C. Rostomily, and E.C. Alvord, *The cause of death in patients with glioblastomas is multifocal: Clinical factors and autopsy findings in 117 cases of supratentorial glioblastomas in adults*, J. Neuro-Oncol. 10 (1991), pp. 179–185.

[13] K.R. Swanson, E.C. Alvord, and J.D. Murray, *A quantitative model for differential motility of gliomas in grey and white matter*, Cell Prolif. 33 (2000), pp. 317–329.

[14] K.R. Swanson, E.C. Alvord, and J.D. Murray, *Virtual brain tumours (gliomas) enhance the reality of medical imaging and highlight inadequacies of current therapy*, Br. J. Cancer 86 (2002), pp. 14–18 [Abstracted and featured in the Year Book of the Institute of Oncology Elsevier Science (2003)].

[15] K.R. Swanson, E.C. Alvord, and J.D. Murray, *Quantifying efficacy of chemotherapy of brain tumors (gliomas) with homogeneous and heterogeneous drug delivery therapy*, Acta Biotheor. 50(4) (2002), pp. 223–237.

[16] K.R. Swanson, E.C. Alvord, and J.D. Murray, *Virtual resection of gliomas: Effect of extent of resection on recurrence*, Math. Comput. Model. 37(11) (2003), pp. 1177–1190.

[17] K.R. Swanson, C. Bridge, J.D. Murray, and E.C. Alvord, *Virtual and real brain tumors: Using mathematical modeling to quantify glioma growth and invasion*, J. Neurol. Sci. 216(1) (2003), pp. 1–10.

[18] K.R. Swanson, R.C. Rostomily, and E.C. Alvord, *A mathematical modelling tool for predicting survival of individual patients following resection of glioblastoma: A proof of principle*, Br. J. Cancer 98 (2008), pp. 113–119.

[19] M. Tafforeau, M.-C. Verdus, V. Norris, G.J. White, M. Cole, M. Demarty, M. Thellier, and C. Ripoll, *Plant sensitivity to low intensity 105 GHz electromagnetic radiation*, Bioelectromagnetics 25 (2004), pp. 403–407.

[20] P. Tracqui, G.C. Cruywagen, D.E. Woodward, G.T. Bartoo, J.D. Murray, and E.C. Alvord, *A mathematical model of glioma growth: The effect of chemotherapy on spatial-temporal growth*, Cell Prolif. 28 (1995), pp. 17–31.

[21] N.D. Volkow, D. Tomasi, G.-J. Wang, P. Vaska, J.S. Fowler, F. Telang, D. Alexoff, J. Logan, and C. Wong, *Effects of cell phone radiofrequency signal exposure on brain glucose metabolism*, JAMA 305(8) (2011), pp. 808–813.

[22] D.E. Woodward, J. Cook, P. Tracqui, G.C. Cruywagen, J.D. Murray, and E.C. Alvord, *A mathematical model of glioma growth: The effect of extent of surgical resection*, Cell Prolif. 29 (1996), pp. 269–288.